Fundamental Axial Spindle Motions And Optical Tolerancing

Mark Craig Gerchman

Rank Taylor Hobson Inc.
Keene, New Hampshire 03431 USA

Abstract

This paper will examine the surface error which results as a consequence of fundamental axial spindle motion in the diamond turning process. A mathematical model of this error will be developed and contrasted with a traditional Zernike error fit. In addition, the effect of this error on the optical performance of these surfaces will be investigated.

Introduction

Recent advances in machine tools for single point diamond turning have significantly improved the quality of machined surfaces. The most recent generation of SPDT lathes are producing optical surfaces suitable for many visible applications. It is beneficial to analyze these surfaces to isolate the sources of residual errors with the view towards further improvement. One source of machine tool error that generates a very unusual surface error is fundamental axial spindle motion.

Fundamental axial spindle motion (FASM) is a well understood machine tool error motion[1] and is described in the national standards[2]. Fundamental axial spindle motion consist of a once-per-revolution axial movement of the work holding spindle. Figure 1 shows the effect of FASM on the scribing of a cylindrical diameter. As the spindle rotates a complete revolution, with an absence of any spindle error motion, the non-influencing scribe would generate a circle (dotted line) on the cylindrical diameter. If the spindle has only a fundamental axial motion then the scribe generates an ellipse (solid line) on the cylinder.

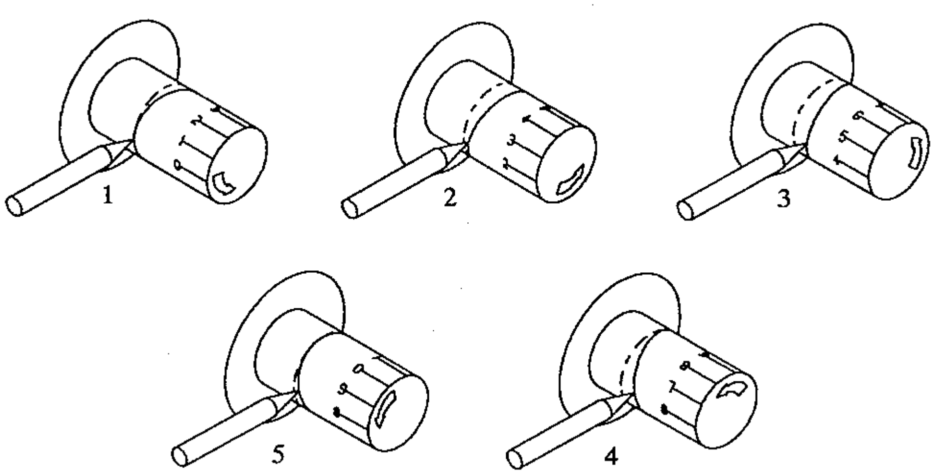

Figure 1 - Fundamental Axial Spindle Motion

[1] Bryan, J.B., Clouser, R.W., and Holland, E., "Spindle Accuracy", *American Machinist*, December 4, 1967.
[2] "Axes of Rotation, Methods for Specifying and Testing", ANSI/ASME B89.3.4M - 1985.

An analytical model for the error created by FASM has some unusual features as relates to traditional optical geometries. Since the spindles motion is fundamental and does not depend on the radial distance from the spindle centerline the sagitta surface error can be expressed as a simple equation. In a cylindrical coordinate system aligned with the spindle motion the equation of surface error is $z = k \sin(\varphi)$: where k is the amplitude of the fundamental axial motion and φ is the azimuthal angle. Figure 2 shows this sagitta error referenced to a surrounding plane. The nature of this error has many consequences in the optical tolerancing of surfaces with this error. Because the error is not a function of radial distance there exist a pole discontinuity at the vertex of the surface. This discontinuity in the paraxial region makes traditional aberration image analysis difficult.

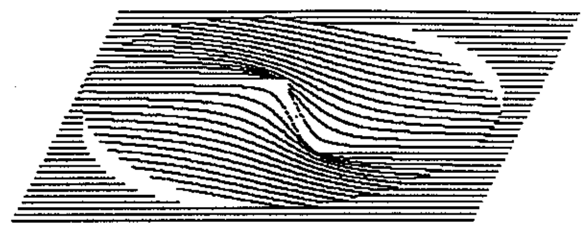

Figure 2 - Surface Error Due To Fundamental Axial Spindle Motion

Zernike Circle Polynomial Fit To FASM

In a traditional sense the fitting of optical fabrication errors is accomplished by the application of Zernike circle polynomials. In addition to orthogonality and invariance over the unit circle, these polynomials are well suited to the evaluation of optical systems because of their numerical similarity with the balancing of optical aberrations of different orders. Although the Zernike's have favorable properties for the representation of traditional wavefronts and surface errors, their ability to accurately represent an unusual surface (*e.g.* a surface error caused by FASM) needs to be examined.

This analysis will be restricted to the use of the lowest 36 Zernike terms since this is the typical number of terms used in most optical aberration tolerancing studies. If the coordinate system used is aligned with the spindle motion, then of these 36 terms only five have the necessary angular dependence to represent this fundamental motion. Equation 1 relates the FASM sagitta error to both the Zernike polynomial and an alternate polynomial constructed of fundamental terms to different radial powers. The relationship between the coefficients of these polynomials is given in Equations 2.

$$z = k\sin(\varphi) = k\begin{pmatrix} a_2\,\rho\,\sin(\varphi)+ \\ a_7\,\rho^3\sin(\varphi)(3\rho^2-2)+ \\ a_{14}\rho^5\sin(\varphi)(10\rho^4-12\rho^2+3)+ \\ a_{23}\rho^7\sin(\varphi)(35\rho^6-60\rho^4+30\rho^2-4)+ \\ a_{34}\rho^9\sin(\varphi)(126\rho^8-280\rho^6+210\rho^4-60\rho^2+5) \end{pmatrix} = k\begin{pmatrix} b_1\rho\,\sin(\varphi)+ \\ b_3\rho^3\sin(\varphi)+ \\ b_5\rho^5\sin(\varphi)+ \\ b_7\rho^7\sin(\varphi)+ \\ b_9\rho^9\sin(\varphi) \end{pmatrix} \tag{1}$$

$$\begin{aligned} b_1 &= a_2 - 2a_7 + 3a_{14} - 4a_{23} + 5a_{34} \\ b_3 &= 3a_7 - 12a_{14} + 30a_{23} - 60a_{34} \\ b_5 &= 10a_{14} - 60a_{23} + 210a_{34} \\ b_7 &= 35a_{23} - 280a_{34} \\ b_9 &= 126a_{34} \end{aligned} \tag{2}$$

Coefficients for the alternate polynomial can be found using the method of least squares. Equation 3 shows the difference in errors between the FASM surface and the alternate polynomial representation at each point on the unit circle.

$$\varepsilon_{\rho,\varphi} = k\sin(\varphi) - k\left[b_1\rho\sin(\varphi) + b_3\rho^3\sin(\varphi) + b_5\rho^5\sin(\varphi) + b_7\rho^7\sin(\varphi) + b_9\rho^9\sin(\varphi)\right] \tag{3}$$

The sum of the squares of all the errors can be found by integrating over the unit circle as shown in Equation 4.

$$E = \int_{\rho=0}^{1} \int_{\varphi=0}^{2\pi} \varepsilon^2 \rho \, \partial\varphi \, \partial\rho \qquad (4)$$

Values for the "b" coefficients can be found by differentiating this total squared error with respect to each of the "b" coefficients and setting these values to zero. This produces a set of five integral equations. Solving these integrals reduces these equations to Equations 5.

$$\begin{array}{lcl} 1/3 & = & b_1/4 + b_3/6 + b_5/8 + b_7/10 + b_9/12 \\ 1/5 & = & b_1/6 + b_3/8 + b_5/10 + b_7/12 + b_9/14 \\ 1/7 & = & b_1/8 + b_3/10 + b_5/12 + b_7/14 + b_9/16 \\ 1/9 & = & b_1/10 + b_3/12 + b_5/14 + b_7/16 + b_9/18 \\ 1/11 & = & b_1/12 + b_3/14 + b_5/16 + b_7/18 + b_9/20 \end{array} \qquad (5)$$

The numerical solution to this set of equations must be performed to many significant digits since the required determinant is ill-conditioned. This signifies that the solution may not provide an adequate representation of the original FASM function. The solution for the "b" coefficients and the equivalent Zernike coefficients are given in Equations 6. Note that the Zernike coefficients have a surprisingly simple generating function.

$$\begin{array}{ll} b_1 = 5.454545 & a_2 = 1.333333 = (1*4)/(3*1) \\ b_3 = -25.454545 & a_7 = -0.533333 = (-2*4)/(5*3) \\ b_5 = 61.090909 & a_{14} = 0.342857 = (3*4)/(7*5) \\ b_7 = -65.454545 & a_{23} = -0.253968 = (-4*4)/(9*7) \\ b_9 = 25.454545 & a_{34} = 0.202020 = (5*4)/(11*9) \end{array} \qquad (6)$$

Figure 3 shows the Zernike circle polynomial fit using these coefficients. The scale of error in the figure is the same as that used for the FASM representation in Figure 1. Although the overall form is similar, there are clearly an insufficient number of terms to fully represent the error. In particular the slope at the vertex of the surface can not, with any reasonable number of Zernike terms, represent the effect of the pole singularity. The alternating signs of the Zernike terms result in the zonal disturbance that can easily be seen towards the edge of the surface. Here the effect of each higher order term is counteracting the effects of the proceeding term. This results in significant slope departures at the surface's edge. Note the absence of these slope errors in the original Figure 1, FASM representation.

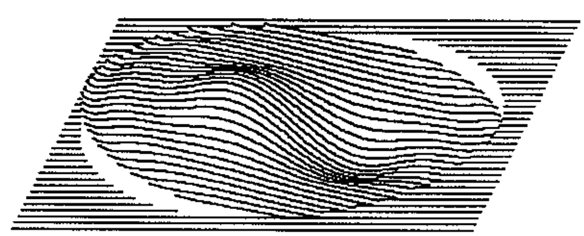

Figure 3 - Surface Errors Due To A Zernike Polynomial Representation

Optical Tolerancing of FASM Surfaces

One technique to evaluate the effects of the FASM error on the optical performance of a surface is to use spot diagrams. In this example geometrical spot diagrams will be produced from a surface with FASM error and the Zernike representation of that error. The surface used has a base shape of an f/1.0 paraboloid of revolution with a 50 mm diameter. The total (peak to valley) FASM error used was 0.1 µm. An on-axis uniform rectilinear grid of just slightly over 4000 rays were traced off of these surfaces. The spot diagrams produced are taken at the paraxial image plane and are shown in Figures 4 and 5.

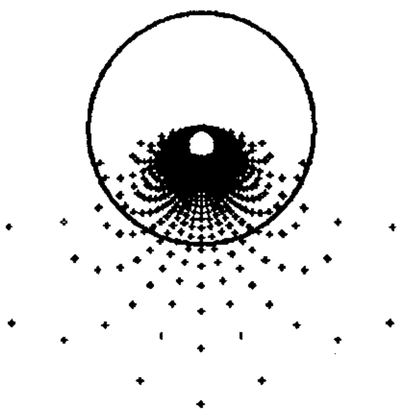

Figure 4 - FASM Surface Error (Spot Diagram)

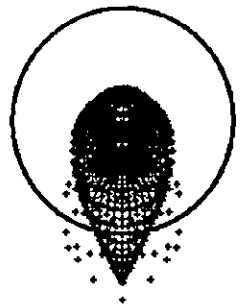

Figure 5 - Zernike Representation (Spot Diagram)

The results of this side-by-side comparison show very clearly how poorly the limited Zernike polynomial represented the FASM error. The circles in both figures represents the first zone of the Airy disk pattern at a wavelength of 632.8 nm. Aside from the skewness of both spot diagrams these figures look very different. The *r.m.s.* spot sizes for the FASM error is less than half that of the Zernike representation. While the Zernike spot shows a clear alternating zone coma structure the FASM spot does not. The FASM spot is dominated by the presence of a few ill-directed rays and a very small central cluster. The central cluster is itself dominated by a zone where there is an absence of any ray intersections! This surprising result is not predicted by the traditional Zernike analysis.

Conclusions

This paper has described fundamental axial spindle motion and described how it can be mathematically modeled for optical tolerance analyses. A description of this error in a traditional Zernike approximation has shown the inadequacy of using these polynomials for such an unusual surface error.

Submitted for presentation at the SIRA Conference on Commercial Applications Of Precision Manufacturing At The Sub-Micron Level, London, United Kingdom, November 19, 1991, SPIE Proceedings Vol. 1573.